JOURNAL OF PROPULSION AND POWER
Vol. 9, No. 4, July–Aug. 1993

Time-Marching Method for the Prediction of Two-Dimensional, Unsteady Flows of Condensing Steam

A. J. White* and J. B. Young†
University of Cambridge, Cambridge CB3 ODY, England, United Kingdom

A time-accurate, two-dimensional time-marching technique is presented which can predict unsteady phenomena in condensing steam flows. Conservation equations for the mixture are solved using a variation of a well-established Euler solver, while nucleation and droplet growth calculations are performed in a Lagrangian framework by tracking particle pathlines. A special averaging technique is used to retain a polydispersion of droplet sizes, necessary for the accurate modeling of the condensation processes, without consuming excessive storage or CPU time. The basic Euler solution technique has been validated by comparison with predictions from an independent source for the unsteady flow of air in a channel. The full scheme has been used to compute nucleating flows in converging-diverging nozzles for which agreement with experiment for both steady and unsteady cases is extremely good. All the results presented are for flows in nozzles for which experimental data are available, but the scheme may also be applied to turbine cascade geometries.

Nomenclature

c_{pg} = isobaric specific heat capacity of vapor
e = specific internal energy
h = specific enthalpy
h_{fg} = specific enthalpy of evaporation
J = nucleation rate per unit volume
k = Boltzmann's constant
l_g = mean free path of vapor molecule
m, m_i = mass of water molecule, mass of group i droplet
n = number of droplets per unit mass of mixture
Pr_g = Prandtl number of vapor
p = pressure
q_c, q_e = condensation and evaporation coefficients
R_g = specific gas constant
r = droplet radius
r^* = Kelvin-Holmholtz critical radius
T = temperature, period of oscillation
t = time
u, v = velocity components
x, y = spatial coordinates
y = wetness fraction
α = droplet growth parameter
γ = ratio of specific heat capacities
ΔT = vapor subcooling
λ_g = thermal conductivity of vapor
ρ = density
σ = surface tension

Subscripts
f = liquid phase
g = vapor phase
i = droplet group i
s = saturation conditions

Superscript
n = time level

Received Oct. 7, 1991; revision received Nov. 4, 1992; accepted for publication Dec. 18, 1992.

*Research Associate, Department of Engineering, Whittle Laboratory, Madingley Road.
†University Lecturer, Department of Engineering, Whittle Laboratory, Madingley Road.

Introduction

THE presence of condensation in the low pressure (LP) stages of steam turbines is known to have an adverse effect on turbine performance, and since it is these stages which produce a large proportion of the power output, there is considerable financial impetus for improving their efficiency. Considerable research into turbines operating with wet steam has therefore been undertaken, but nevertheless, most design procedures still adopt a single-phase approach combined with an empirical correlation[1] to account for wetness effects. Recently, the use of optical wetness probes[2] has enabled the performance of individual stages operating with wet steam to be measured. These measurements have indicated that it is usually the stage in which condensation first occurs that demonstrates the lowest efficiency, and further, that the magnitude of the associated loss appears to vary with the location of condensation onset (i.e., with the degree of turbine inlet superheat). This should be a source of optimism for researchers, since it implies that the high levels of loss associated with wetness are not necessarily inevitable.

It has been suggested[3] that the occurrence of oscillating flow regimes as a result of the release of latent heat during condensation may be a contributing factor towards the poor performance of some LP stages. These regimes involve the formation, migration, and collapse of an aerodynamic shock wave within the condensation zone and were first observed by Schmidt[4] for the flow of moist air. An explanation of their behavior was later given by Barschdorff and Fillipov[5] who also attempted to predict their frequency using a quasi-steady theoretical model. To date, however, observation and prediction of these oscillations have been confined to converging-diverging nozzles in which the flow is essentially one-dimensional, and whether such phenomena occur in the three-dimensional environment of a steam turbine remains to be properly investigated. However, if this were so, the consequences would be twofold:

1) The periodic quenching of nucleation by the moving shock wave would result in larger water droplets than would otherwise be produced (thus giving rise to larger thermodynamic and mechanical losses).

2) The existence of the oscillating shock wave itself might have an adverse effect on blade aerodynamics.

This article presents a two-dimensional time-marching technique for computing the unsteady nonequilibrium flow of wet

steam with a view to investigating the type of unsteadiness described above. All the results presented here are for flows in channels or convering-diverging nozzles, but the method is readily extendable to turbine cascade geometries. The solution procedure uses a strategy similar to previous methods for two-dimensional wet-steam calculations[6,7] and involves the Lagrangian tracking of fluid particles for the calculation of nucleation and droplet growth combined with the solution of the mixture conservation equations in an Eulerian framework. The method described here, however, is the first to be based on a time-accurate Euler solver and also to incorporate tracking in two dimensions of particle pathlines rather than streamlines. It is therefore suitable for the accurate investigation of unsteady phenomena. (It is necessary to distinguish between streamlines and pathlines for the case of unsteady flow. Streamflows are lines which are parallel to the velocity vectors at every point in the flow at a given instant, whereas pathlines define the trajectory of a fluid particle as its position varies with time. Streamlines and pathlines become coincident for steady flow.)

Basic Equations

The equations governing the flow of wet steam have been presented many times in the literature and are reproduced here in outline only for completeness.

Wet steam is assumed to be a mixture of vapor at T_g, p, and ρ_g, with a large number of spherical liquid droplets. In reality, there will be a continuous distribution of droplet sizes, but for the present calculations this has been discretized into a finite number of droplet groups. The ith group contains n_i droplets per unit mass of mixture, each of r_i and T_i. The liquid density ρ_f is assumed constant.

The overall wetness fraction y of the mixture is the sum of the contributions from the individual groups, given by

$$y = \Sigma y_i = \Sigma n_i m_i = \Sigma \tfrac{4}{3}\pi r_i^3 \rho_i n_i \tag{1}$$

The mixture density is related to the vapor density by

$$\frac{1}{\rho} = \frac{1-y}{\rho_g} + \Sigma \frac{y_i}{\rho_i} \approx \frac{1-y}{\rho_g} \tag{2}$$

where the approximation follows if the volume of the liquid phase is neglected. The specific internal energy of the mixture is

$$e = (1-y)e_g + \Sigma y_i e_i \tag{3}$$

where e_g is evaluated at T_g, and e_i is the specific internal energy of an ith group droplet, including a contribution from the surface energy

$$e_i = e_i' + \frac{3}{\rho_i r_i}\left(\sigma_i - T_i \frac{d\sigma_i}{dT_i}\right)$$

e_i' being the specific internal energy of bulk liquid evaluated at T_j. The mixture specific enthalpy is given by a similar expression.

In general, the two phases are not in equilibrium, so T_g and T_i differ from T_s. The vapor subcooling is defined as

$$\Delta T = T_s - T_g \tag{4}$$

and Gyamarthy's approximation is used for the temperature of the liquid phase

$$T_i = T_s - \Delta T_i \tag{5}$$

where ΔT_i is the capillary subcooling associated with group i droplets, given by

$$\Delta T_i = \frac{2\sigma_i T_s}{\rho_i h_{fg} r_i} \tag{6}$$

For the very small droplets formed by spontaneous nucleation, velocity slip between the vapor and liquid phases may be neglected. With this approximation, the Euler equations for the inviscid, adiabatic, compressible flow of the mixture become identical to their single-phase counterparts

continuity

$$\frac{\partial \rho}{\partial t} + \nabla\cdot(\rho \boldsymbol{u}) = 0 \tag{7}$$

momentum

$$\frac{\partial \boldsymbol{u}}{\partial t} + (\boldsymbol{u}\cdot\nabla)\boldsymbol{u} + \frac{\nabla p}{\rho} = 0 \tag{8}$$

energy

$$\frac{\partial(\rho E)}{\partial t} + \nabla\cdot(\rho \boldsymbol{u} H) = 0 \tag{9}$$

where E and H are the specific energy and specific total enthalpy of the mixture, defined in the normal fashion as $E = e + u^2/2$ and $H = h + u^2/2$.

For single-phase flow, Eqs. 7–9 are closed by means of thermal and caloric equations of state. For wet steam, however, the closure requires, in addition, an expression for the wetness fraction which is obtained from the theories of nucleation and droplet growth.

Nucleation

For the present calculations, the rate of formation of critically sized embryos per unit volume of mixture J is given by steady-state classical nucleation theory[8] with a correction for nonisothermal effects, as proposed by Kantrowitz[9]

$$J = \frac{1}{1+\phi} q_c \sqrt{\left(\frac{2\sigma_g}{\pi m^3}\right)} \frac{\rho_g^2}{\rho_f} \exp\left(-\frac{4\pi r^{*2}\sigma_g}{3kT_g}\right) \tag{10}$$

where ϕ is the nonisothermal correction factor

$$\phi = 2\frac{\gamma-1}{\gamma+1}\frac{h_{fg}}{R_g T_g}\left(\frac{h_{fg}}{R_g T_g} - \frac{1}{2}\right)$$

and r^* is the Kelvin-Helmholtz critical radius

$$r^* = \frac{2\sigma_g T_s}{\rho_f h_{fg} \Delta T} \tag{11}$$

The liquid surface tension σ_g is evaluated at the vapor temperature.

Assuming zero interphase velocity slip, the values of the n_i (the number of droplets per unit mass of mixture in group i) remain constant once nucleation has terminated (except, of course, in regions of complete re-evaporation).

It should be stressed that there still remains some controversy over the exact form of the nucleation rate equation with other theories (e.g., the "gasification factor" modification[10]) giving nucleation rates that differ by several orders of magnitude from that of Eq. (10). In addition, inspection of Eq. (10) reveals the strong dependence of the nucleation rate on surface tension. (Since r^* is proportional to σ^2, the exponent contains the third power of σ. Typically, 1% decrease in σ

would increase the nucleation rate by a factor of 2.) Various corrections have been proposed for the surface tension of small clusters of molecules (e.g., Tolman[11]), but these are at best approximate. For the present work the flat film value of σ has been adopted and only its variation with temperature has been taken into account. Nucleation rates computed in this way are then in close agreement with the many experiments in nozzles, expansion chambers, and diffusion cloud chambers reported in the literature.

As a fluid particle traverses the flowfield, it sees a continuous variation of subcooling, which, in accordance with Eqs. (10) and (11), results in the formation of nuclei of different radii, which subsequently grow at different rates. It is therefore important to retain a spectrum of droplet sizes in the calculations if nucleation and growth are to be modeled accurately. However, it is very expensive in terms of both computer storage and computation time to retain all the droplet groups. Therefore, groups which are of very similar radii are replaced with a single group containing the same mass of liquid and total number of droplets. More groups are retained in the smaller droplet size range since, owing to their greater specific surface area, these droplets play a more active role in the interphase heat and mass transfer.

Droplet Growth

The overall growth rate of the liquid phase is found by summing contributions from the individual droplet groups. Noting that $m_i = 4\pi r_i^3 \rho_f/3$ and differentiating (1) yields

$$\frac{Dy}{Dt} = \Sigma \frac{Dy_i}{Dt} = \Sigma \frac{3y_i}{r_i} \frac{Dr_i}{Dt} \tag{12}$$

where D/Dt is the rate of change following a fluid particle (i.e., the substantive derivative).

Equation (12) neglects the contribution from freshly nucleated droplets. (This is a good approximation since nucleation is assumed to occur at the critical radius.)

The rate of growth of a group i droplet Dr_i/Dt is dictated by the rate at which the enthalpy of phase change can be conducted to the surrounding vapor. The growth law adopted here is a modified form of that due to Gyarmarthy[12]

$$(h_g - h_i) \frac{Dr_i}{Dt} = \frac{\lambda_g (T_i - T_g)}{\rho_f [r_i + 1.89(1 - \nu)(l_g/Pr_g)]} \tag{13}$$

where ν is given by

$$\nu = \frac{R_g T_g}{h_{fg}} \left(\alpha - 0.5 - \frac{2 - q_c}{2q_c} \frac{\gamma + 1}{2\gamma} \frac{c_{pg} T_s}{h_{fg}} \right)$$

The factor $(1 - \nu)$ and the corresponding parameter α were suggested by Young[13] who noted that agreement between experiments in steam nozzles and calculations based on the unmodified Gyarmathy equation tended to deteriorate for Wilson Point pressures below 0.5 bar. Furthermore, it proved impossible to restore agreement by a simple adjustment to the nucleation rate equation alone. The parameter α reflects the fact that q_c and q_e are not necessarily equal under conditions of nonequilibrium droplet growth. At present, the kinetic theory of the liquid state is not sufficiently well-developed to provide a theoretical estimate of the value of α, which must therefore be regarded as a parameter to be determined empirically. However, it should be appreciated that the disagreement between theory and experiment, even with the usual assumption of $\alpha = 0$ (i.e., $q_c = q_e$), is not dramatic and that variations in the correction factor $(1 - \nu)$ have no qualitative effect on the results and conclusions of this article.

Introducing Eqs. (5), (6), and (11) into Eq. (13) gives (after some minor approximations)

$$(h_g - h_i) \frac{Dr_i}{Dt} = \frac{\lambda_g \Delta T [1 - (r^*/r_i)]}{\rho_f [r_i + 1.89(1 - \nu)(l_g/Pr_g)]} \tag{14}$$

This equation shows that the droplet growth rate is inextricably linked with the vapor subcooling ΔT, the determination of which is now described.

Equations (8) and (9) are combined to give the Lagrangian form of the energy equation

$$\frac{Dh}{Dt} = \frac{1}{\rho} \frac{Dp}{Dt} \tag{15}$$

[For nonequilibrium flow, Eq. (15) does not imply that the entropy of a fluid particle remains constant. The neglect of viscosity and thermal conductivity in the momentum and energy conservation Eqs. (8) and (9) ensures zero entropy production due to velocity and temperature gradients in the vapor phase. This however, does not preclude the possibility of entropy generation due to irreversible droplet growth, because the droplets are considered as sources and sinks of heat and mass distributed uniformly throughout the vapor and their temperature is, in general, different from that of their surroundings. This aspect of the mathematical modeling procedure is discussed by Marble.[25] The situation is similar to other cases in relaxation gas dynamics as described by Becker.[26]] Incorporating an expression similar to Eq. (3) for the mixture enthalpy and applying standard thermodynamic relations then yields

$$\frac{D(\Delta T)}{Dt} = \frac{DT_s}{Dt} - \frac{1}{c_{pg}} \Sigma \frac{D}{Dt} [y_i (h_g - h_i)] + \frac{1}{c_{pg}} \left(\frac{1 - \alpha_g T_g}{\rho_g} - \Sigma \frac{y_i}{\rho_i} \right) \frac{Dp}{Dt} \tag{16}$$

where α_g is the coefficient of thermal expansion of the vapor

$$\alpha_g = -\frac{1}{\rho_g} \left(\frac{\partial \rho_g}{\partial T_g} \right)_p$$

Equations (12), (14), and (16) together enable the wetness fraction to be calculated and, with a suitable equation of state for the vapor phase, complement the Euler equations for the mixture variables.

The fact that low-pressure steam behaves as an imperfect gas is accurately accounted for by the use of an equation of state which includes an empirical expression for the compressibility parameter $Z\{p, T_g\}$ defined such that $p = [1 + Z\{p, T_g\}]\rho_g R_g T_g$. Thermodynamically consistent expressions relate all the other vapor phase properties and details of these, along with the form of $Z\{p, T_g\}$, are given by Young.[7]

Numerical Solution of Equations

The computational grid employed is of the widely used H mesh variety, consisting of quadrilaterals formed by the intersection of quasiorthothogonals (lines of constant x) with quasistreamlines. Refinement of the mesh is made in regions where condensation is expected to occur. For symmetrical nozzles, calculations are performed on a grid spanning just one-half of the width of the nozzle.

Solution of Euler Equations

The Euler Eqs. (7–9) may be recast in integral form as

$$\frac{\partial}{\partial t} \int \boldsymbol{U}\, dx\, dy + \int \{\boldsymbol{F}\, dy - \boldsymbol{G}\, dx\} = 0 \tag{17}$$

where

$$\boldsymbol{U} = \begin{bmatrix} \rho \\ \rho u \\ \rho v \\ \rho E \end{bmatrix}, \quad \boldsymbol{F} = \begin{bmatrix} \rho u \\ \rho u^2 + p \\ \rho uv \\ \rho uH \end{bmatrix}, \quad \boldsymbol{G} = \begin{bmatrix} \rho v \\ \rho uv \\ \rho v^2 + p \\ \rho vH \end{bmatrix}$$

Equation (17) is marched forward in time using a second-order-accurate Runge-Kutta algorithm. The scheme used is essentially the same as that of Jameson et al.,[14] but differs in the following respects:

1) Properties are stored at cell vertices and the control volumes are as depicted in Fig. 1. Fluxes across a face of a control volume are evaluated by averaging quantities stored at its two ends and the calculated changes in flow properties within the cells are distributed equally to the four vertices, thus preserving spatial symmetry.

2) In order to preserve time accuracy for unsteady calculations, a global time step is employed rather than local time steps pertaining to the stability limits of the individual cells.

3) The adaptive blend of second- and fourth-order dissipative terms proposed by Jameson is retained in the streamwise direction but has been replaced in the transverse direction by a constant second-order smoothing as used by Denton.[15] This is because, for a symmetrical nozzle calculation, typically only 5–10 grid points are required across the half-width, and a fourth-order differencing routine would become preoccupied with extrapolating differences at the flow boundaries. In addition, some numerical difficulties have been reported on the use of Jameson-style smoothing with cell vertex schemes.[16]

A four-step scheme has been found to be robust and computationally efficient and this takes the form

$$
\begin{aligned}
\boldsymbol{U}^{(1)} &= \boldsymbol{U}^n - a_1\Delta t\{\tfrac{1}{4}(\boldsymbol{R}_{i,j} + \boldsymbol{R}_{i-1,j} + \boldsymbol{R}_{i-1,j-1} \\
&\quad + \boldsymbol{R}_{i,j-1})^n + \boldsymbol{D}^n_{i,j}\} \\
\boldsymbol{U}^{(2)} &= \boldsymbol{U}^n - a_2\Delta t\{\tfrac{1}{4}(\boldsymbol{R}_{i,j} + \boldsymbol{R}_{i-1,j} + \boldsymbol{R}_{i-1,j-1} \\
&\quad + \boldsymbol{R}_{i,j-1})^{(1)} + \boldsymbol{D}^n_{i,j}\} \\
\boldsymbol{U}^{(3)} &= \boldsymbol{U}^n - a_3\Delta t\{\tfrac{1}{4}(\boldsymbol{R}_{i,j} + \boldsymbol{R}_{i-1,j} + \boldsymbol{R}_{i-1,j-1} \\
&\quad + \boldsymbol{R}_{i,j-1})^{(2)} + \boldsymbol{D}^n_{i,j}\} \\
\boldsymbol{U}^{n+1} &= \boldsymbol{U}^n - a_4\Delta t\{\tfrac{1}{4}(\boldsymbol{R}_{i,j} + \boldsymbol{R}_{i-1,j} + \boldsymbol{R}_{i-1,j-1} \\
&\quad + \boldsymbol{R}_{i,j-1})^{(3)} + \boldsymbol{D}^n_{i,j}\}
\end{aligned}
\tag{18}
$$

where $a_1 = 0.25$, $a_2 = 0.333$, $a_3 = 0.5$, and $a_4 = 1.0$. The $\boldsymbol{R}_{i,j}$ are the residuals in cell (i, j) (see Fig. 1), calculated by summing the fluxes into the cell and dividing by its area, and the $\boldsymbol{D}^n_{i,j}$ are the dissipative terms (evaluated at the first step only) added to stabilize the scheme and prevent overshoots in the neighborhood of shock waves.

At the inlet boundary, specific entropy and total enthalpy are specified and the pressure is extrapolated from the interior. At the outflow boundary, the temperature and velocity components are extrapolated from the interior. For supersonic outflow the pressure is extrapolated, whereas for subsonic outflow it is specified.

Nucleation and Droplet Growth Calculations

Since the time derivatives of Eqs. (14) and (16) are all substantive, these equations are most conveniently solved by integrating along fluid pathlines. For this purpose, the velocity field obtained by solution of the Euler equations is used to determine the instantaneous trajectories of fluid particles. The procedure is illustrated in Fig. 2. Point Q represents a computational node in the new time plane $(n + 1)$, and point P, in the old time plane n, is the origin of a fluid particle subsequently arriving at Q. The position of P is estimated by tracking backwards in time from Q and is then corrected by a single iteration.

Examination of Eq. (16) reveals that the droplet spectrum (and hence, the wetness fraction) at Q is completely specified by the original spectrum and subcooling at P, together with the pressure variation as a function of time along PQ. The relevant properties at P are found using a four-point interpolation routine which is based on transforming the quadrilateral cells into squares. (This is a trivial matter for the H mesh upon which the present calculations are based.)

In order to determine the variation of pressure along PQ, an estimate of the pressure at Q is required. This is obtained by first expressing the vapor phase equations of state in differential form

$$
\mathrm{d}p = \left(\frac{\partial p}{\partial \rho_g}\right)\mathrm{d}\rho_g + \left(\frac{\partial p}{\partial T_g}\right)\mathrm{d}T_g
$$

$$
\mathrm{d}e_g = \left(\frac{\partial e_g}{\partial \rho_g}\right)\mathrm{d}\rho_g + \left(\frac{\partial e_g}{\partial T_g}\right)\mathrm{d}T_g
$$

Combining these two equations readily gives an expression relating changes in pressure to changes in density and specific internal energy of the vapor. These changes may be interpreted as variations in time at a fixed point in space (i.e., between Q' and Q), and are therefore provided by the Euler solver in conjunction with expressions (2) and (3). Hence, it is possible to estimate the pressure at Q. The variation along PQ is prescribed by assuming a constant expansion rate, $-\mathrm{D}(\ell_n p)/\mathrm{D}t$, between P and Q. [It will be noted that the above procedure requires knowledge of the wetness fraction y at Q. In the present calculations, old values of y (i.e., at Q') have been used, but numerical experiments have been conducted using values of y corrected by a first-order difference for $\partial y/\partial t$. These produced identical results, suggesting that a more sophisticated approach is unnecessary.]

The numerical integration of the nucleation and droplet growth equations is performed using straightforward predictor-corrector routines which are contained within a wet-steam "black box," originally developed by Guha and Young[17] and later modified by Young.[7] One advantage of this black box is that it only relates thermodynamic states of the two-phase mixture, requiring no knowledge of the velocity field. It can thus be incorporated into any one- two- or three-dimensional

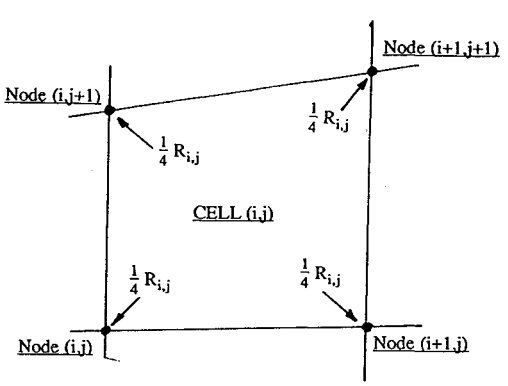

Fig. 1 Computational control volume and distribution of residuals.

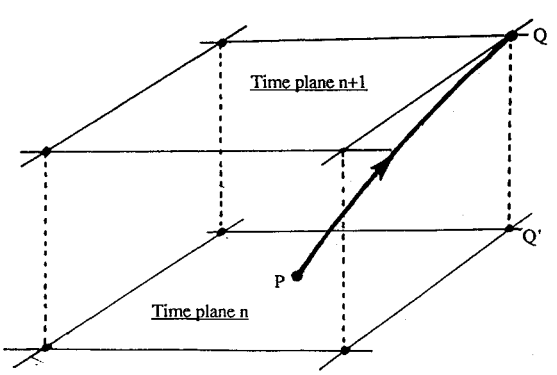

Fig. 2 Fluid particle pathline.

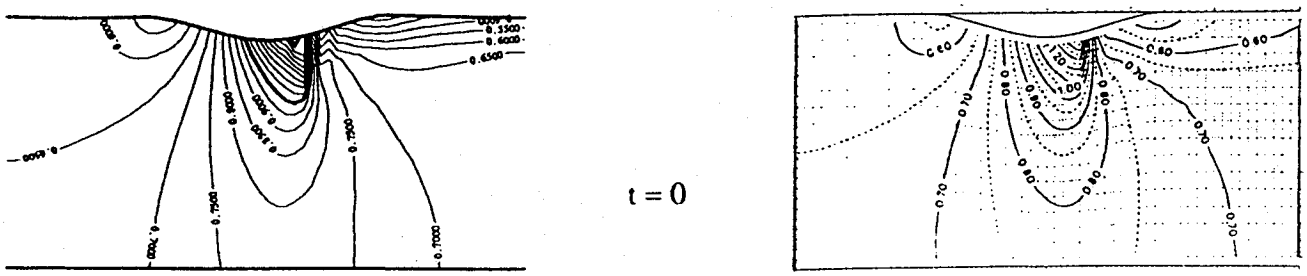

Flow Direction

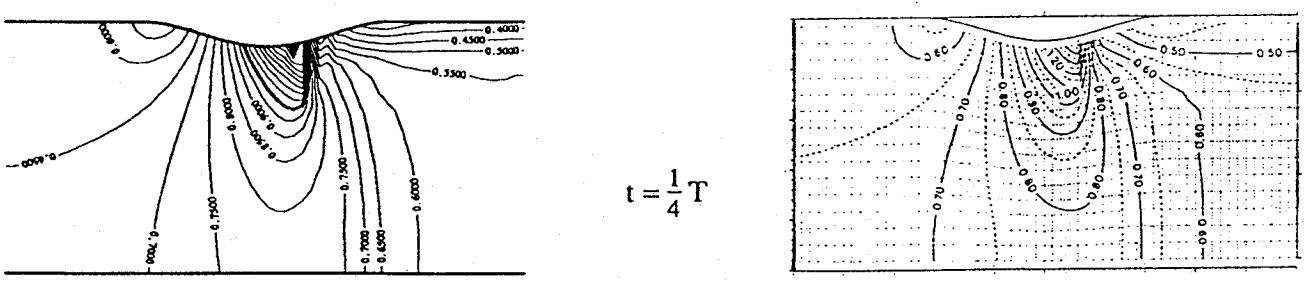

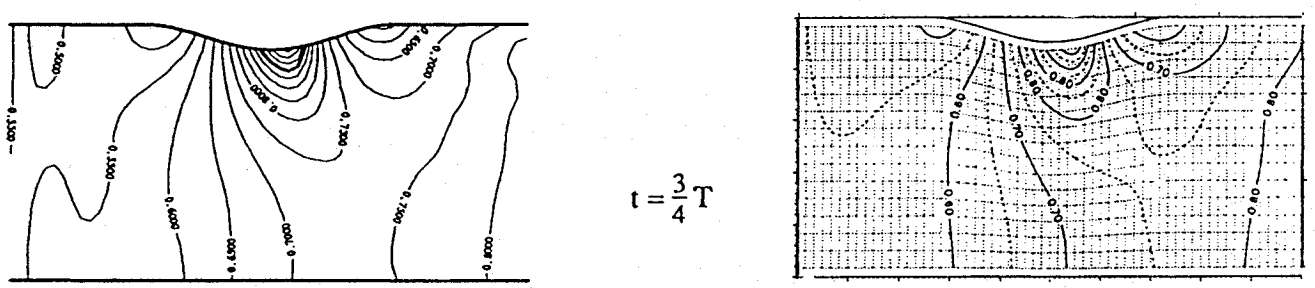

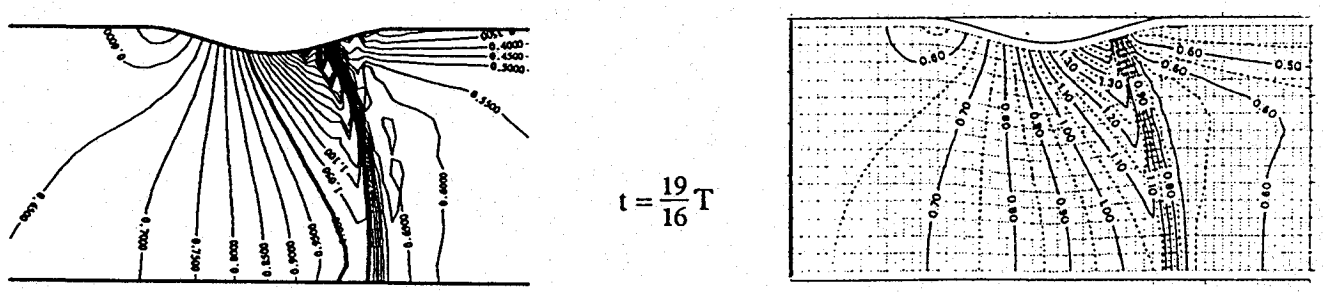

Interval = 0.05
Sonic lines in bold

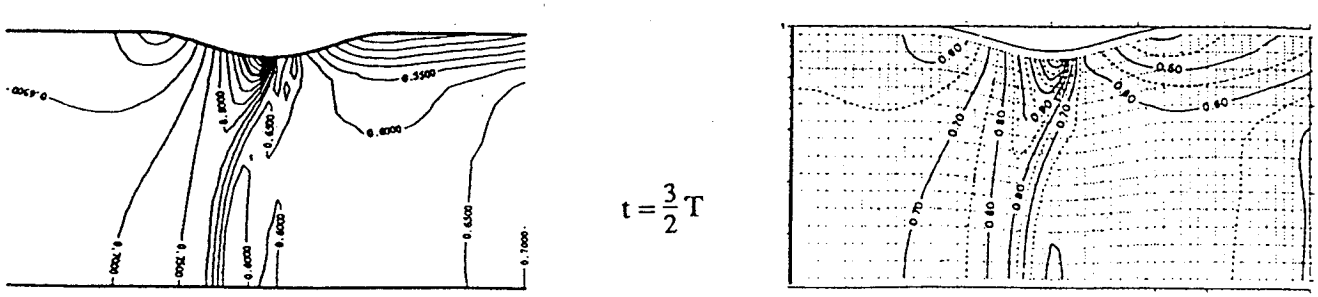

Current Theory

Grid = 61x15

Theory of Bölcs et al. (ref. 18).

Fig. 3 Mach number contours for unsteady flow of air over a bump.

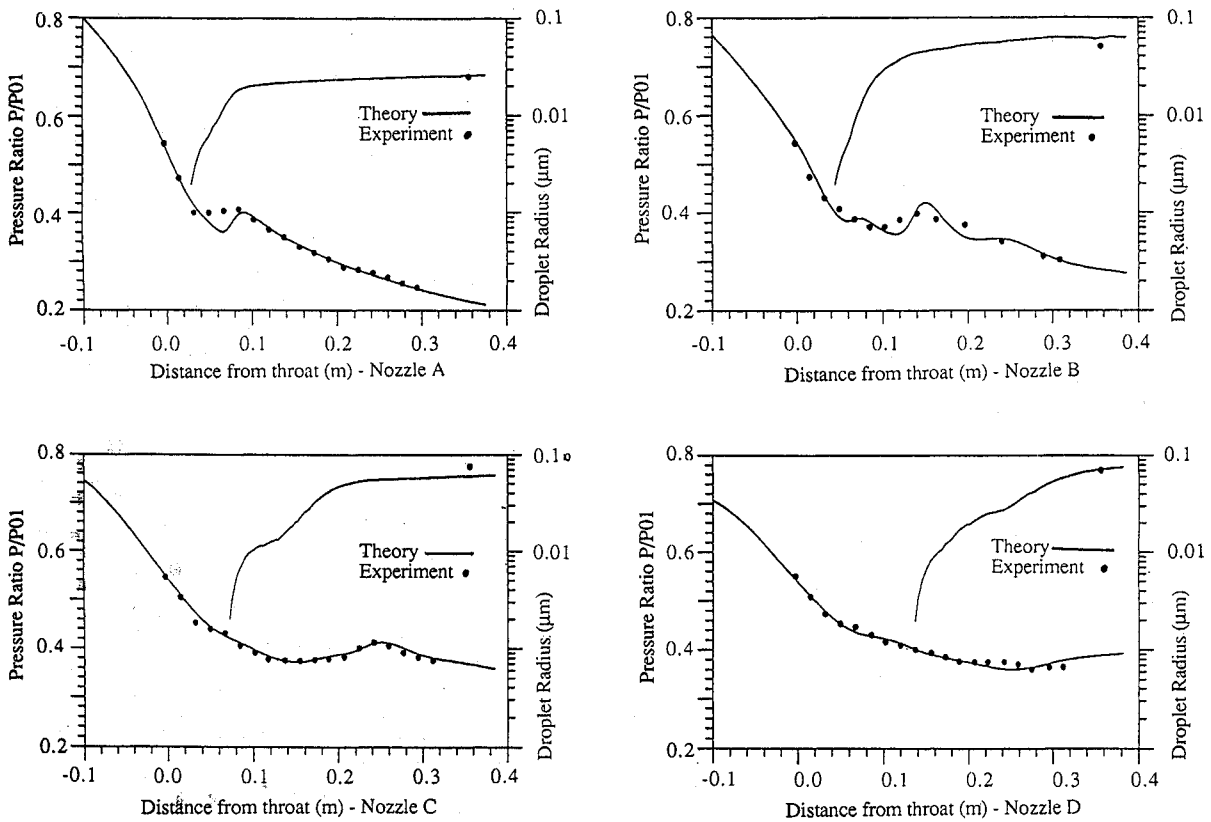

Fig. 4 Condensation in converging-diverging nozzles—comparison with experiments of Moore et al.[22]

steady or unsteady flow solver, according to application. The only required inputs are the initial conditions and the pressure-time variation of a fluid particle, in this case obtained as described above.

Examples of Application

Transonic Flow of Air with Fluctuating Back Pressure

Before attempting to apply the method to condensing flows of steam, various tests were carried out to validate the basic Euler solver. That presented here is for the flow of air over a hump in a channel. Unsteadiness is induced by a sinusoidal variation of the back pressure, with an amplitude of 12% of inlet stagnation pressure and a frequency of 369 Hz [corresponding to a reduced frequency ($a_0 f/L$) of 5.31, where L is the channel length, f the true frequency, and a_0 the stagnation speed of sound based on the inlet stagnation temperature]. The nature, amplitude, and frequency of shock oscillations in this case bear great resemblance to those induced by condensation in nozzles. This is, therefore, an excellent test of the suitability of the Euler solver as a basis for predicting unsteady condensation phenomena.

The results are compared in Fig. 3 with calculations of the same flow by Bölcs et al.[18] using a flux vector splitting scheme. (In this figure, T stands for the period of oscillation $1/f$.) This scheme, in turn, has been validated against linear theory for smaller amplitude oscillations. Despite the considerably greater simplicity of the present method, the predictions of Mach number contours are very similar. For a description and physical explanation of the flow pattern at the various stages in the cycle, the reader is referred to the paper by Bölcs et al.[18]

Steady Condensation in Steam Nozzles: Experimental Comparison

If dry steam with an inlet stagnation state near the saturation line is expanded through a converging-diverging nozzle, its subcooling may eventually reach a level (typically 30–40°C) sufficient to induce significant spontaneous nucleation. In laboratory nozzle tests this occurs in the supersonic part of the

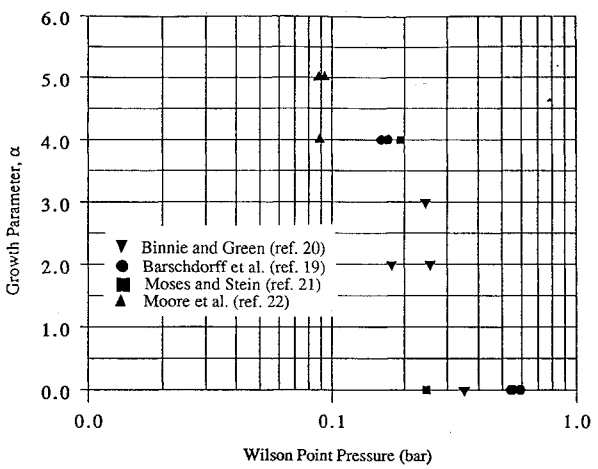

Fig. 5 Variation of droplet growth parameter α[13] with Wilson point pressure.

flow, since subsonic expansions from a dry stagnation state are unable to provide the required subcooling. The effect of the condensation heat release may override the effects of the area increase, causing a deceleration of the flow and a corresponding increase in pressure. Traditionally, this pressure rise has been termed the "condensation shock" but, as long as the heat release is not great enough to decelerate the flow to sonic conditions (i.e., the subcritical regime), variations are in fact continuous. (Strictly speaking, this is only true in the context of a one-dimensional flow approximation, since in real two- and three-dimensional flows the possibility of oblique shock waves means that discontinuities may exist in an entirely supersonic flowfield.)

Numerous measurements have been made of the pressure distribution in nozzles for condensing steam.[19–21] However, Young[13] has pointed out that the success of nucleation and droplet growth theories can only be assessed separately if both

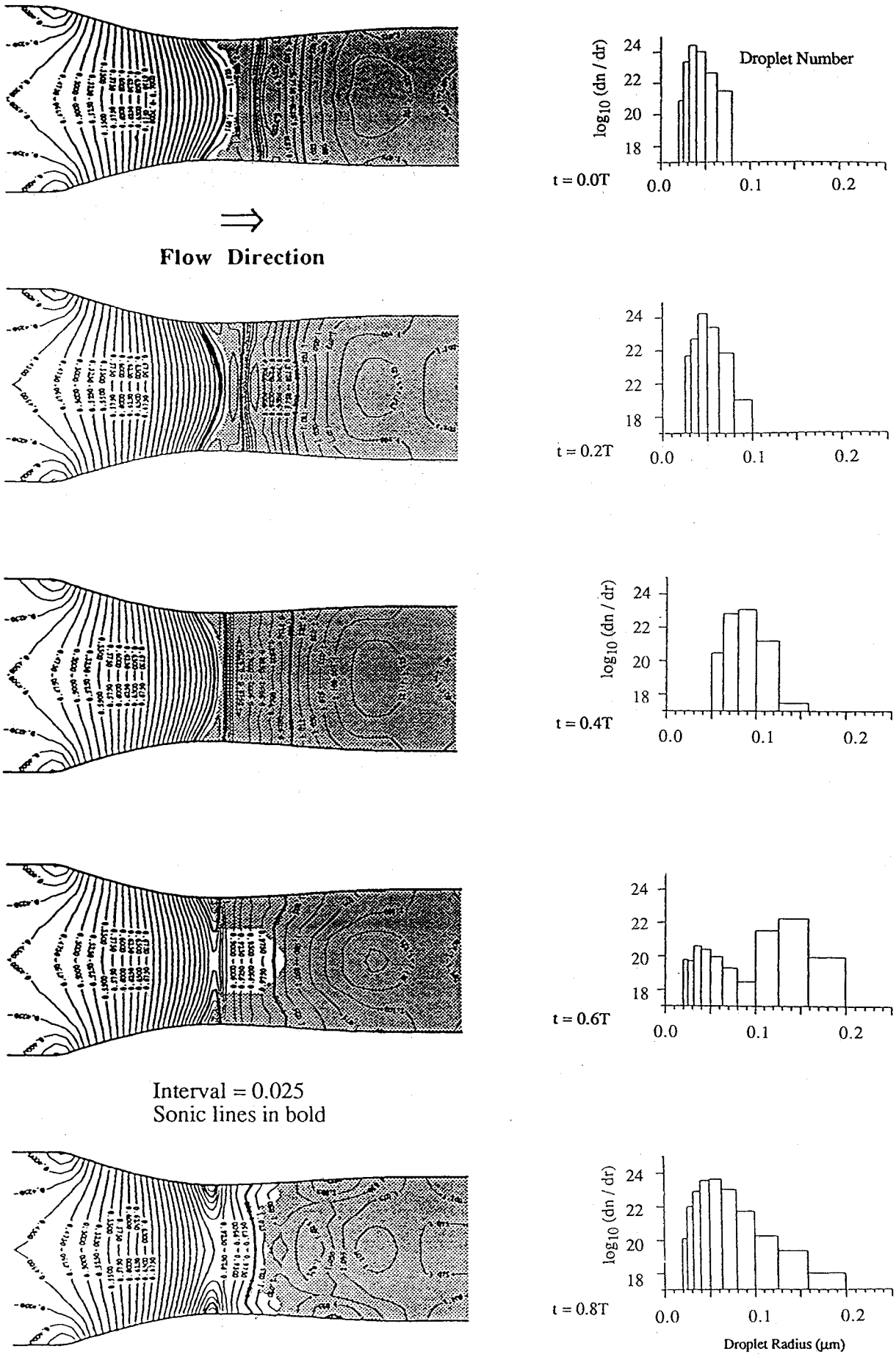

Fig. 6a Frozen Mach number contours and droplet number spectra for unsteady condensation in the nozzle of Skillings et al.[3]

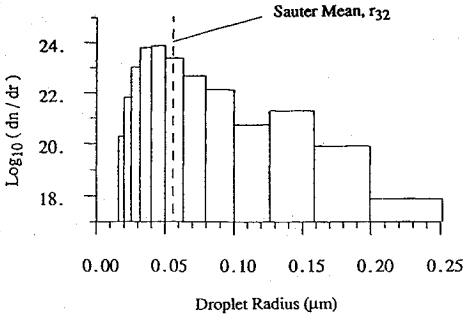

Fig. 6b Time-averaged droplet number spectrum for nozzle of Fig. 6a.

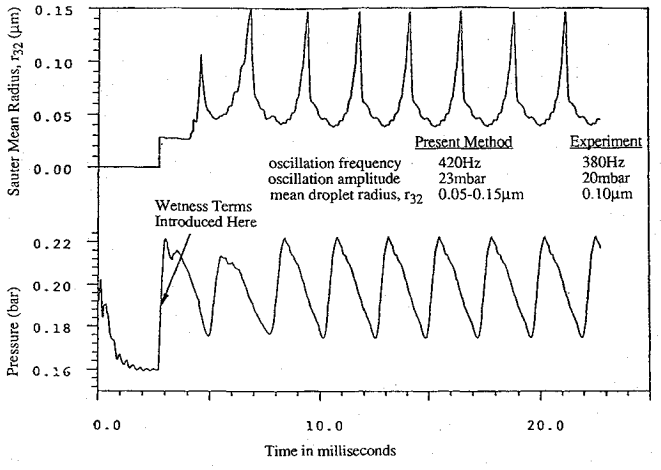

Fig. 6c Pressure and droplet size fluctuations for nozzle of Fig. 6a.

pressure variation and droplet size measurements are available, and unfortunately, such measurements are much less abundant. Those of Moore et al.,[22] however, are particularly relevant to LP steam turbine conditions, and these are presented in Fig. 4 along with predictions from the current theory. The mean droplet sizes and pressure distributions are very well-predicted in all cases, with the possible exception of nozzle *B*. It is interesting to note that the flow in some of these nozzles is quite strongly two-dimensional. The evidence for this is the undulations in centerline pressure distribution, which are particularly pronounced for nozzle *B*. The significance of these two-dimensional effects (which have also been verified using the method of characteristics for perfect gas flow) is that the varying expansion rates will strongly influence the position of maximum subcooling, and hence, the final droplet size. A two-dimensional calculation scheme is therefore liable to predict quite a different droplet size distribution from a one-dimensonal approach. Unfortunately, the two-dimensionality makes it much more difficult to take account of boundary layers, and this may explain the lack of agreement in the case of nozzle *B*. (It is customary to infer the effective nozzle area from the pressure distribution of a completely dry expansion. This technique is valid when the flow is effectively one-dimensional because the pressure distribution is then only a function of the area ratio. However, it is difficult to take account of the boundary layers when the flow exhibits two-dimensional features without a thorough knowledge of the displacement thickness variation.)

In view of the comments made in preceding sections about the uncertainties surrounding nucleation and droplet growth theories, some degree of calibration of the equations is necessary. In accordance with the work of Young,[13] this is achieved through variation of q_c and the parameter α in the expression following Eq. (13). Since recent experimental work has indicated that the condensation coefficient for water is unlikely to differ substantially from unity, all the calculations were performed with $q_c = 1$, while α was allowed to vary. Figure 5 shows the values of α required to give best agreement with a number of experiments reported in the literature covering a range of Wilson point pressures between 0.1–1.0 bar. Due to experimental uncertainty, these values do not form a smooth curve, but the trend is clear. Figure 5 was therefore used as a "calibration graph" in order to obtain a value of α for the calculations of unsteady flow presented below.

Unsteady Supercritical Condensation

If the level of heat release from condensation is more than sufficient to revert the flow to sonic conditions (i.e., the supercritical regime), then an adiabatic shock wave establishes itself within the condensation zone. In situations where the heat release is particularly large, the shock wave may be unable to locate a stable position and thus migrates upstream where it interacts with the nucleation zone. The increase in temperature through the shock wave results in a suppression of nucleation, and hence, the subsequent heat release (and thereby the reason for the shock wave's existence) dies away. A supersonic expansion with attendant condensation is then re-established and the process repeats itself, giving rise to self-sustained oscillations.

Figure 6a shows the Mach number contours (based on the frozen speed of sound) predicted by the present method for oscillations of the type described above. The sonic lines ($M = 1$) have been highlighted for clarity, and regions containing significant condensed liquid are indicated by shading. Also shown in Fig. 6a are the droplet number spectra, as would be seen by a probe situated on the centerline, near the nozzle exit, where near-equilibrium conditions, constant pressure, and hence, constant wetness fraction prevail. These spectra have been plotted at times approximately $0.1T$ (where T is the period of oscillation) later than the adjacent contour plots, the difference being the time of flight of fluid particles between the nucleation zone at the throat and the "probe" in the exit plane.

At the beginning of the cycle ($t = 0$), there are three sonic lines corresponding to choking at the geometric throat, deceleration through a supercritical shock wave, and subsequent re-acceleration to supersonic conditions. Nucleation occurs rapidly over a very small region near the throat, so the droplet number distribution is almost monodispersed. At $t = 0.2T$, the shock wave has moved upstream, but has not yet reached the nucleation zone, so there is little change in the droplet spectrum. At $t = 0.4T$, the shock wave begins to interact with the nucleation zone, the temperature increase suppressing the formation of nuclei. In order to achieve the same downstream equilibrium wetness fraction, the smaller number of droplets must grow to a larger size, as shown by the change in the droplet spectrum. By $t = 0.6T$, the shock wave is passing through the throat, and has become so weak as to be entirely subsonic (a shock wave may still be maintained in the flow since, due to its movement, the upstream relative conditions are still supersonic). Two supersonic patches remain near the nozzle walls and these are consistent with the structures observed by Schnerr[23] for the flow of moist air, in which two incipient shocks were accompanied by an unsteady central portion. The residual condensation, formed before the arrival of the shock wave, has now been convected away leaving a dry region just downstream of the throat, and a new nucleation front begins further downstream. The droplet spectrum is thus bimodal, consisting of large droplets originating from nucleation near the throat, and smaller droplets originating from the new nucleation front. Finally, at $t = 0.8T$, the large droplets have been convected out of the nozzle completely and the new condensation front begins to dominate. The droplet spectrum therefore reverts to a monomodal form.

The time-averaged droplet size distribution is plotted in Fig. 6b and is seen to be slightly bimodal. Evidence of bimodality has been observed in optical measurements in LP steam tur-

bines,[24] but is much stronger than that shown in Fig. 6b, which would not be detectable with an optical probe. Unsteady phenomena of this type are thus unlikely to be the sole cause of the bimodal droplet distributions found in turbines.

The results presented in Figs. 6a and 6b are for the nozzle of Skillings et al.,[3] for which experimental measurements of fluctuating pressure and mean droplet size were made at points on the nozzle centerline. Predictions of these quantities are shown in Fig. 6c, where it can be seen that the amplitude of the pressure fluctuation and the computed mean droplet size variation compare very favorably with the measured values. Furthermore, the predicted frequency of 420 Hz compares well with the measurement of 380 Hz. Previous predictions for this particular experiment include the one-dimensional pseudounsteady calculations of Skillings et al.[3] which gave a frequency of ~650 Hz, and the fully unsteady one-dimensional calculations of Guha and Young[17] which gave a frequency of ~540 Hz. The contours of Fig. 6a, however, indicate that the flow is markedly two-dimensional and this accounts for the improved accuracy of the present method.

Conclusions

A time-accurate two-dimensional time-marching technique has been described and used to predict both steady and unsteady flows of condensing steam in nozzles. Agreement with experimental results is very good in terms of pressure distributions, droplet sizes, and frequency of oscillation. The technique is computationally efficient requiring, e.g., approximately 5 min per cycle of oscillation for the nozzle of Fig. 6 on a grid of 64 × 7 nodes, using an Alliant FX-80 computer. By retaining a polydispersion of droplet sizes the calculations accurately model the condensation process. This is particularly relevant to unsteady condensing flows where, as shown in Fig. 6a, secondary nucleation results in a bimodal droplet size distribution.

The comparisons of calculations with experimental results serve mainly as a validation of the computer code and scarcely demonstrate its two-dimensional capability. With some minor extensions, however, the code will provide a valuable tool for investigating flows in steam turbine blade passages, where the complex interaction between condensation and blade aerodynamics is not at present well understood.

References

[1]Baumann, K., "Some Recent Developments in Large Steam Turbine Practice," *Journal of the Institution of Electrical Engineers*, Vol. 59, 1921, p. 565.

[2]Walters, P. T., "Wetness and Efficiency Measurements in LP Turbines with an Optical Probe as an Aid to Improving Performance," joint American Society of Mechanical Engineers/Inst. of Electrical and Electronic Engineers Conf. on Power Generation, Paper 85-JPGC-GT-9, Milwaukee, WI, Oct. 1985.

[3]Skillings, S. A., Moore, M. J., Walters, P. T., and Jackson, R., "A Reconsideration of Wetness Loss in LP Steam Turbines," *Proceeding of the BNES (British Nuclear Energy Society), Conference on Technology of Turbine Plant Operating with Wet Steam,* London, 1988, pp. 171–177.

[4]Schmidt, B., "Beobachtungen über das Verhalten der durch Wasserdampfkondensation ausgelösten Störungen in einer Überschall-Windkanaldüse," Ph.D Dissertation, Univ. of Karlsruhe (TH), Germany, 1962.

[5]Barschdorff, D., and Fillipov, G. A., "Analysis of Certain Special Operating Modes of Laval Nozzles with Local Heat Supply," *Heat Transfer—Soviet Research*, Vol. 2, No. 5, 1970, pp. 76–87.

[6]Moheban, M., and Young, J. B., "A Time-Marching Method for the Calculation of Blade-to-Blade Nonequilibrium Wet Steam Flows in Turbine Cascades," Inst. of Mechanical Engineers, Conf. on Computational Methods in Turbomachinery, Univ. of Birmingham, Paper C76/84, Birmingham, England, UK, 1984, pp. 89–99.

[7]Young, J. B., "Two-Dimensional Nonequilibrium Wet Steam Calculations for Nozzles and Turbine Cascades," *Transactions of the American Society of Mechanical Engineers Journal of Turbomachinery*, Vol. 114, 1992, pp. 569–579.

[8]MacDonald, J. E., "Homogeneous Nucleation of Vapour Condensation," *American Journal of Physics*, Pt. 1, Vol. 30, 1962–63, pp. 870–877; Pt. 2, Vol. 131, pp. 31–41.

[9]Kantrowitz, A., "Nucleation in Very Rapid Expansions," *Journal of Chemical Physics*, Vol. 19, No. 9, 1951, pp. 1097–1100.

[10]Feder, J., Russell, K. C., Lothe, J., and Pound, G. M., "Homogeneous Nucleation and Growth of Droplets in Vapours," *Advances in Physics*, Vol. 15, 1966, pp. 111–178.

[11]Tolman, R. C., "The Effect of Droplet Size on Surface Tension," *Journal of Chemical Physics*, Vol. 17, 1949, pp. 333–337.

[12]Gyarmarthy, G., "Two-Phase Steam Flow in Turbines and Separators," edited by M. J. Moore, and C. H. Sieverding, Hemisphere, Washington, DC, 1976, pp. 163–168.

[13]Young, J. B., "The Spontaneous Condensation of Steam in Supersonic Nozzles," *Physico Chemical Hydrodynamics*, Vol. 3, No. 1, 1982, pp. 57–82.

[14]Jameson, A., Schmidt, W., and Turkel, E., "Numerical Solution of the Euler Equations by Finite Volume Methods Using Runge-Kutta Time Stepping Schemes," AIAA 14th Fluid and Plasma Dynamics Conf., AIAA Paper 81-1259, Palo Alto, CA, June 1981.

[15]Denton, J. D., "An Improved Time-Marching Method for Two- and Three-Dimensional Blade to Blade Flows," *Journal of Engineering for Power*, Vol. 105, 1983, pp. 514–524.

[16]He, L., "An Euler Solution of Unsteady Flows Around Oscillating Blades," American Society of Mechanical Engineers Gas Turbine and Aeroengine Congress and Expo., Paper 89-GT-279, Toronto, Canada, June 1989.

[17]Guha, A., and Young, J. B., "Time-Marching Prediction of Unsteady Condensation Phenomena Due to Supercritical Heat Addition," *IUTAM Symposium on Adiabatic Waves in Liquid-Vapour Systems*, edited by G. E. A. Meier, and P. A. Thompson, Göttingen, Germany, 1989, Springer-Verlag, 1991, pp. 159–170.

[18]Bölcs, A., Fransson, T. H., and Platzer, M. F., "Numerical Solution of Inviscid Transonic Flow Through Nozzles with Fluctuating Back Pressure," *Transactions of the American Society of Mechanical Engineers Journal of Turbomachinery*, Vol. 111, 1989, pp. 169–180.

[19]Barschdorff, D., Hausmann, G., and Ludwig, A., "Flow and Drop Size Investigations of Wet Steam at Sub- and Supersonic Velocities with the Theory of Homogeneous Condensation," 3rd Conf. on Steam Turbines of Great Output, Gdansk, Poland, Sept. 1974; see also *PIMP* (*Trans. Institute of Fluid-Flow Machinery*), Polish Acad. Sci., Vols. 70–72, 1976, pp. 241–257.

[20]Binnie, A. M., and Green, J. R., "An Electrical Detector of Condensation in High Velocity Steam," *Proceedings of the Royal Society (UK), A*, Vol. 181, 1943, p. 134.

[21]Moses, C. A., and Stein, G. D., "On the Growth of Steam Droplets Formed in a Laval Nozzle Using Both Static Pressure and Light Scattering Measurements," *Journal of Fluids Engineering*, Vol. 100, 1978, pp. 311–322.

[22]Moore, M. J., Walters, P. T., Crane, R. I., and Davidson, B. J., "Predicting the Fog Drop Size in Wet Steam Turbines," Inst. of Mechanical Engineers (UK), Wet Steam 4 Conf., Univ. of Warwick, Paper C37/73, 1973.

[23]Schnerr, G., "Homogene Kondensation in Stationären Transsonischen Strömungen Durch Lavaldüsen und um Profile," Ph.D. Dissertation, Univ. Karlsruhe (TH), Germany, 1986, p. 50.

[24]Walters, P. T., "Improving the Accuracy of Wetness Measurements in Generating Turbines by Using a New Procedure for Analysing Optical Transmission Data," *Proceedings of the BNES (British Nuclear Energy Society), Conference on Technology of Turbine Plant Operating with Wet Steam*, London, 1988, pp. 207–215.

[25]Marble, F. E., "Some Gas Dynamic Problems in the Flow of Condensing Vapours," *Astronautica Acta*, Vol. 14, 1969, pp. 585–614.

[26]Becker, E., "Relaxation Effects in Gas Dynamics," *Aeronautical Journal of the Royal Aeronautical Society*, Vol. 74, 1970, pp. 736–748.